available at www.sciencedirect.com

ScienceDirect

www.elsevier.com/locate/brainres

BRAIN RESEARCH

Research Report

Effects of minocycline on Na^+ currents in rat dorsal root ganglion neurons

Tae Hoon Kim[a], *Hong Im Kim*[a], *Jungho Kim*[b], *Mijung Park*[c], *Jin-Ho Song*[a,*]

[a]*Department of Pharmacology, College of Medicine, Chung-Ang University, Seoul 156-756, Republic of Korea*
[b]*Laboratory of Molecular and Cellular Biology, Department of Life Science, Sogang University, Seoul 121-742, Republic of Korea*
[c]*Department of Visual Optics, Seoul National University of Science and Technology, Seoul 139-743, Republic of Korea*

ARTICLE INFO

Article history:
Accepted 9 November 2010
Available online 4 December 2010

Keywords:
Dorsal root ganglion
Minocycline
Na^+ current
Tetracycline
Tetrodotoxin-resistant
Tetrodotoxin-sensitive

ABSTRACT

Minocycline is an inhibitor of microglial activation and proliferation. Minocycline suppresses pain-related behaviors in many different pain states, which correlates closely with its inhibition of microglial activation and subsequent release of pro-inflammatory mediators in the spinal cord. Na^+ channels in dorsal root ganglion (DRG) neurons are implicated in the generation of inflammatory and neuropathic pain. To elucidate a possible peripheral mechanism of minocycline analgesia, effects of minocycline on tetrodotoxin-sensitive and tetrodotoxin-resistant Na^+ currents in rat DRG neurons were investigated. Minocycline potently inhibited both types of Na^+ currents with IC_{50} values of 350 nM and 410 nM, respectively. The inhibition was accompanied by a depolarizing shift of the activation voltage. However, minocycline slowed the inactivation and speeded up the recovery from inactivation. These results suggest minocycline may exert analgesia peripherally thorough Na^+ channel inhibition in the primary afferent neurons as well as centrally through microglial inhibition in the spinal cord.

1. Introduction

Minocycline, a second-generation semi-synthetic tetracycline, has biological effects distinct from its antimicrobial action. It crosses the blood–brain barrier (Colovic and Caccia, 2003) and has neuroprotective properties against many neurodegenerative diseases such as Huntington's disease, Parkinson's disease, Alzheimer's disease, amyotrophic lateral sclerosis, multiple sclerosis and ischemia (Blum et al., 2004; Stirling et al., 2005; Yong et al., 2004). Inflammation is implicated as a critical mechanism for the pathogenesis of these diseases, and activated microglia mediate much of the inflammatory response in the central nervous system that, ultimately, compromises neuronal viability (Block and Hong, 2005). Minocycline prevents microglial activation and thereby reduces the release of pro-inflammatory mediators, such as interleukin-1β (IL-1β), nitric oxide (NO) and prostaglandin E_2, which are associated with cell death (Domercq and Matute, 2004; Yrjänheikki et al., 1999). Minocycline also interferes with apoptotic cascade and directly blocks neuronal cell death.

Minocycline's anti-inflammatory properties prompted its use in the treatment of rheumatoid arthritis, and the Minocycline in Rheumatoid Arthritis (MIRA) trial revealed minocycline improved clinical symptoms, including joint tenderness (Tilley et al., 1995). Minocycline modulates the function of various molecules and cells implicated in the pathogenesis of

* *Corresponding author*. Department of Pharmacology, College of Medicine, Chung-Ang University, 221 Heuksuk-Dong, Dongjak-Gu, Seoul 156-756, Republic of Korea. Fax: +82 2 817 7115.
E-mail address: jinhos@cau.ac.kr (J.-H. Song).

0006-8993/$ – see front matter © 2010 Elsevier B.V. All rights reserved.
doi:10.1016/j.brainres.2010.11.038

inflammatory arthritis. In particular, minocycline inhibits human synovial collagenase from rheumatoid tissue, both in vivo and in vitro (Greenwald et al., 1987); phospholipase A_2, by interacting with the substrate (Pruzanski et al., 1992); T cell proliferation, and production of IL-2, interferon-γ (IFN-γ) and tumor necrosis factor-α (TNF-α) (Kloppenburg et al., 1995); and NO synthases induced by IL-1β, lipopolysaccharide, or IFN-γ, at the level of RNA expression and translation of the enzyme (Amin et al., 1996).

Both a neuropathic pain induced by sciatic nerve ligation and a formalin-induced inflammatory pain activate spinal cord microglia, and a single intrathecal injection of activated microglia can cause thermal hyperalgesia in naive mice (Cho et al., 2006; Narita et al., 2006). In various pain models minocycline suppresses pain behaviors, and this correlates closely with its inhibition of microglial activation and subsequent pro-inflammatory cytokine release in the spinal cord (Gu et al., 2004; Ledeboer et al., 2005; Raghavendra et al., 2003; Zanjani et al., 2006). Moreover, minocycline reduces both c-Fos positive cells in the spinal dorsal horn and paw edema induced by formalin injection (Cho et al., 2006).

Voltage-gated Na^+ channels play a critical role in regulating primary afferent neuron excitability. Changes in the expression, distribution, and/or function of Na^+ channels in these neurons can lead to chronic neuropathic and inflammatory pain (Amir et al., 2006; Cummins et al., 2007). Of the nine Na^+ channel α-subunits, tetrodotoxin-sensitive (TTX-S) $Na_V1.1$, $Na_V1.6$ and $Na_V1.7$, and tetrodotoxin-resistant (TTX-R) $Na_V1.8$ and $Na_V1.9$ are expressed in dorsal root ganglion (DRG) neurons (Black et al., 2004; Goldin, 2001). $Na_V1.7$, $Na_V1.8$ and $Na_V1.9$ are predominantly expressed in nociceptive neurons, and are closely associated with the development of an abnormal pain state (Akopian et al., 1996; Cummins et al., 2007; Dib-Hajj et al., 1998; Djouhri et al., 2003).

Studies have mostly explained minocycline's analgesic activity in the context of its inhibition of microglial activation in the spinal cord. Moreover, Cho et al. (2006) showed that minocycline inhibited the synaptic currents of substantia gelatinosa neurons in the spinal dorsal horn but not the electrical properties of DRG neurons. However, we have observed that minocycline quite potently inhibits both TTX-S and TTX-R Na^+ currents in rat DRG neurons. This suggests that minocycline may reduce pain peripherally through inhibition of Na^+ currents in sensory neurons.

2. Results

2.1. *Effects of minocycline on Na^+ currents in rat DRG neurons*

TTX-S and TTX-R Na^+ currents in rat DRG neurons were separately recorded using the method described in section 4.2. After establishing a whole-cell configuration, neurons were voltage-clamped at −80 mV. Na^+ currents were evoked by means of depolarizing step pulses to 0 mV at 15-s intervals. Examples of TTX-S and TTX-R Na^+ current traces are shown in Fig. 1A and B, respectively. Activation and inactivation kinetics of the TTX-S Na^+ current were much faster than those of the TTX-R Na^+ current were. Minocycline inhibited both peak Na^+ currents almost equally, and the effects were reversible (Fig. 1C). Minocycline (300 nM) for 10 min inhibited TTX-S Na^+ current to 60±4% of the control (n=7) and TTX-R Na^+ current to 62±4% of the control (n=7). After a 10 min washout, TTX-S and TTX-R Na^+ currents recovered to 92±8% and 87±7% of the control, respectively.

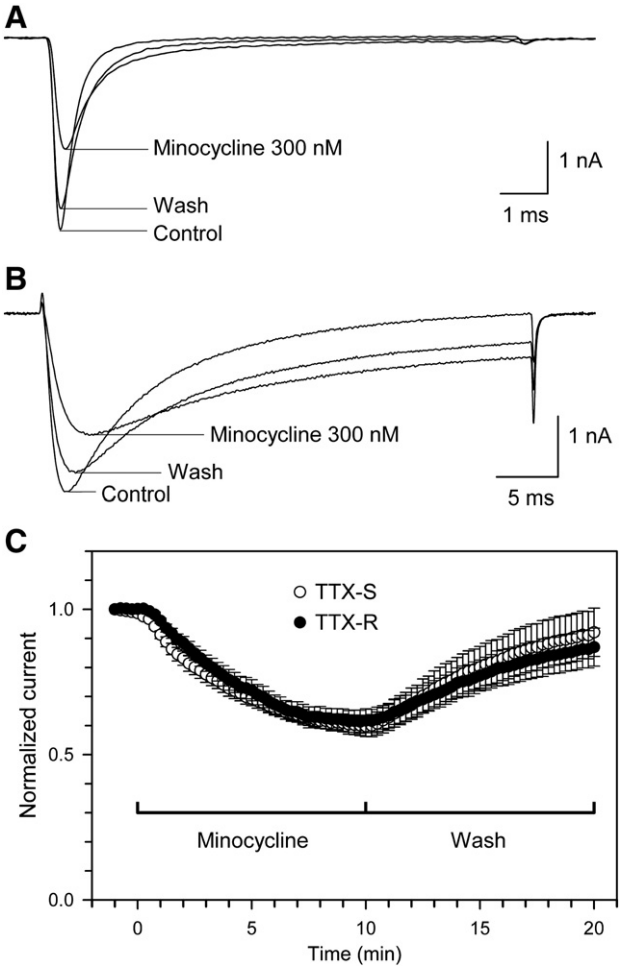

Fig. 1 – Minocycline inhibition of Na^+ currents in rat dorsal root ganglion neurons. (A, B) Typical TTX-S (A) and TTX-R (B) Na^+ current traces before and after 10 min minocycline (300 nM) treatment, and after 10 min of washout. Currents were elicited by depolarizing steps of 10-ms (A) or 40-ms (B) duration to 0 mV from a holding potential of −80 mV at 15-s intervals. (C) Time course of Na^+ current inhibition by minocycline (TTX-S, n=7; TTX-R, n=7).

Minocycline not only reduced the peak currents but also slowed their inactivation (Fig. 1A and B). Inactivation time constant was obtained by fitting the decay phase of the current trace to a single exponential function. At 0 mV, the time constant was 0.40±0.01 ms for TTX-S Na^+ current (n=7) and 8.25±0.54 ms for TTX-R Na^+ current (n=7). After treatment with minocycline (300 nM), they increased to 0.81±0.03 ms (P<0.001) and 17.34±2.51 ms (P<0.01), respectively.

The dose–response relationship for minocycline inhibition of peak Na^+ currents was measured (Fig. 2). Depolarizing step pulses to 0 mV from a holding potential of −80 mV were employed to generate Na^+ currents. Peak currents were

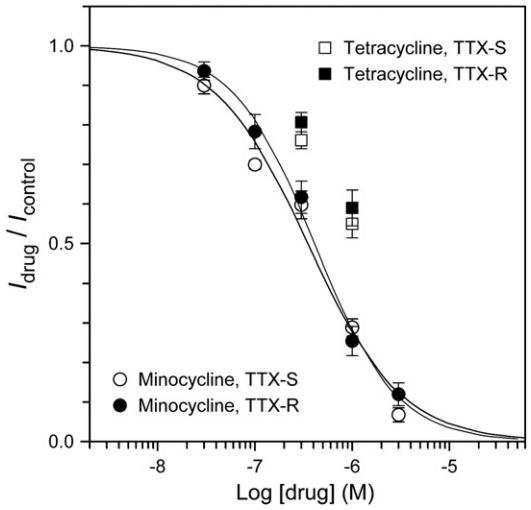

Fig. 2 – Dose–response relationship of the Na^+ current inhibition by minocycline and tetracycline. Peak current amplitude at a 10 min application of drugs (I_{drug}) was normalized to the control current ($I_{control}$), and plotted against the drug concentration. Every measurement was carried out in a different cell (n=7-9). The means of the data were fitted with the Hill equation, to yield smooth lines.

measured in the absence and presence of minocycline for 10 min. Data were collected from 7 to 9 different cells for each minocycline concentration. The mean values of the peak current fraction were fitted with the following Hill equation:

$$I_{minocycline} / I_{control} = 1/\left\{1 + ([minocycline]/IC_{50})^{h}\right\}$$

where $I_{minocycline}$ is peak current in the presence of minocycline, $I_{control}$ is the control peak current, [minocycline] is the minocycline concentration, IC_{50} is the half-maximal inhibitory concentration, and h is the Hill coefficient. Best fits were achieved when IC_{50} and h were 350 nM and 0.91, respectively, for TTX-S Na^+ current, and 410 nM and 1.04, respectively, for TTX-R Na^+ current. Tetracycline also inhibited Na^+ currents but less potently than minocycline did (Fig. 2).

2.2. *Effects of minocycline on the activation of Na^+ currents*

Activation curves were constructed with the membrane potential held at −90 mV (TTX-S) or −80 mV (TTX-R) and the application of a series of test pulses to voltages ranging from −55 to +50 mV, in 5-mV increments at 5-s intervals. Fig. 3A and B show examples of the current families for TTX-S and TTX-R Na^+ currents, respectively, in the absence and presence of minocycline (500 nM) for 10 min.

The peak Na^+ current at each membrane potential was plotted to form current–voltage (I–V) curves (Fig. 3C). The current activation threshold was approximately −45 mV for TTX-S Na^+ current and −30 mV for TTX-R Na^+ current. The maximal inward current occurred at approximately −15 mV and −10 mV, respectively, which shifted in the positive direction after minocycline treatment. The reversal potential for both types of Na^+ currents was approximately +28 mV, which was close to the equilibrium potential calculated from the intracellular and extracellular Na^+ concentrations. Minocycline did not change the reversal potential, implying that minocycline did not interfere with the Na^+ selectivity of the channels.

The current inhibition by minocycline was voltage dependent (Fig. 3D). In both types of Na^+ currents, the inhibition strengthened as membrane potential increased, up to −30 mV for TTX-S current and −15 mV for TTX-R current, but it then weakened as membrane potential increased further.

The voltage-dependent Na^+ current conductance (G) was calculated with the following equation:

$$G = I/(V_m - V_{rev})$$

where I is the peak Na^+ current for each test pulse potential (V_m) and V_{rev} is the reversal potential. G was fitted using the following Boltzmann equation:

$$G/G_{max} = 1/\left\{1 + \exp\left[(V_{1/2} - V_m)/k\right]\right\}$$

where G_{max} is the maximal conductance at +20 mV, $V_{1/2}$ is the membrane potential at half-maximal conductance and k is the slope factor.

Minocycline produced a depolarizing shift in the conductance-voltage (G-V) curve and increased the slope factor in both types of Na^+ currents (Fig. 3E). In TTX-S Na^+ current, $V_{1/2}$ and k were calculated to be −28.0±1.8 mV and 6.14±0.21 mV, respectively (n=9). After 10 min minocycline (500 nM) treatment, they changed by 6.8±0.3 mV and 2.66±0.10 mV, respectively, which differed significantly from the time-dependent, spontaneous changes in the solvent (DMSO 0.1%, v/v), i.e., −3.7±0.7 mV (P<0.001) and 0.20±0.28 mV (P<0.001), respectively (n=7). In TTX-R Na^+ current, $V_{1/2}$ and k were −14.1±0.9 mV and 4.80±0.22 mV, respectively (n=7). In the presence of minocycline (500 nM for 10 min), they changed by 4.3±0.5 mV and 1.85±0.24 mV, respectively, which differed significantly from the spontaneous shifts of −1.7±0.7 mV (P<0.001) and 0.42±0.24 mV (P<0.01), respectively (n=8).

2.3. *Effects of minocycline on the steady-state inactivation of Na^+ currents*

The voltage dependence of steady-state inactivation was estimated by measuring the peak current amplitude elicited by a test pulse to 0 mV after a 10-s pre-pulse to potential over the range of −120 to −40 mV. Fig. 4A and B show typical families of TTX-S and TTX-R Na^+ currents, respectively, before and after treatment with 500 nM minocycline for 10 min. Minocycline reduced the maximal TTX-S and TTX-R Na^+ current elicited from the most hyperpolarized pre-pulse potentials by 47±4% and 46±3%, respectively.

For construction of the steady-state inactivation curve, normalized peak Na^+ current was plotted against the pre-pulse potential (Fig. 4C), and fitted with a Boltzmann function according to the equation:

$$I/I_{max} = 1/\left\{1 + \exp\left[(V_h - V_{1/2})/k\right]\right\}$$

where I is the current amplitude, I_{max} is the maximal current amplitude elicited from the most hyperpolarized pre-pulse potential, V_h is the pre-pulse potential, $V_{1/2}$ is the membrane potential at half-maximal I, and k is the slope factor.

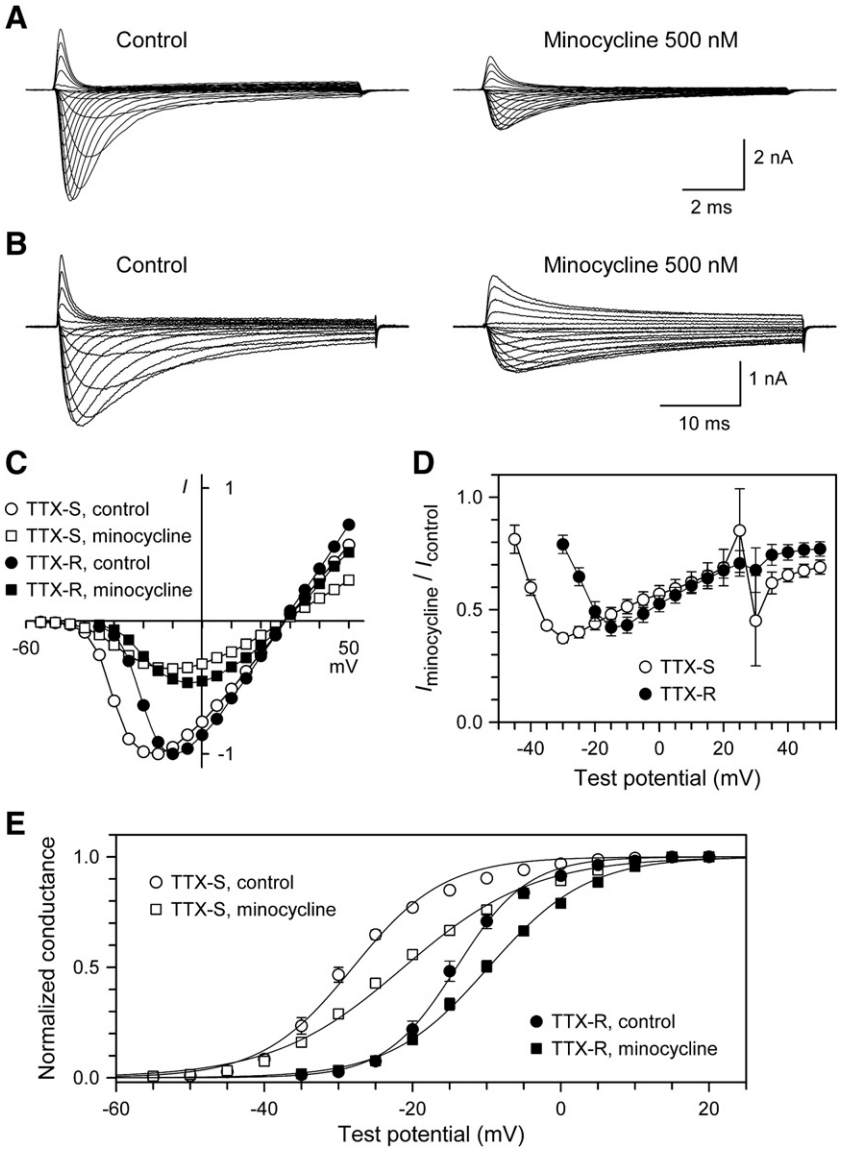

Fig. 3 – Effect of minocycline on the voltage dependency of Na^+ current activation. Membrane potential was held at −90 mV (A) or −80 mV (B), and currents were evoked with test pulses (A, 10 ms; B, 40 ms) to potentials ranging from −55 mV to +50 mV in 5-mV increments. (A, B) Examples of TTX-S (A) and TTX-R (B) Na^+ current families before and after 10 min treatment with minocycline (500 nM). (C) Normalized current–voltage (*I–V*) relationships for the currents shown in panels A and B. (D)Voltage-dependence of minocycline inhibition of Na^+ currents. Currents after treatment with minocycline ($I_{minocycline}$) were normalized to the control current ($I_{control}$). (E) Conductance-voltage (*G-V*) relationships derived from *I–V* data. Conductance was normalized with respect to the maximal conductance at +20 mV and plotted against the test potential (TTX-S, *n* = 9; TTX-R, *n* = 7). Curves were drawn after fit with a Boltzmann function.

The $V_{1/2}$ and *k* for TTX-S Na^+ current were calculated to be −83.7 ± 1.2 mV and 6.41 ± 0.24 mV, respectively (*n* = 8). After treatment with minocycline (500 nM) for 10 min, they changed by 1.1 ± 0.6 mV and 1.42 ± 0.17 mV, respectively. These changes were small but differed statistically from the spontaneous changes of −2.6 ± 0.3 mV ($P < 0.001$) and 0.27 ± 0.16 mV ($P < 0.001$), respectively (*n* = 7). For the TTX-R Na^+ current, the $V_{1/2}$ and *k* were −52.0 ± 1.1 mV and 4.77 ± 0.18 mV, respectively (*n* = 8). In the presence of minocycline (500 nM) for 10 min, they changed by −0.9 ± 0.4 mV and 1.77 ± 0.32 mV, respectively, which differed statistically from the spontaneous changes of −2.6 ± 0.7 mV ($P < 0.05$) and 0.47 ± 0.23 mV ($P < 0.01$), respectively (*n* = 7).

2.4. *Effects of minocycline on the recovery of Na^+ currents from inactivation*

Recovery of Na^+ currents from inactivation was assessed using a two-pulse protocol and varying the inter-pulse duration. Holding potential and inter-pulse potential were both −100 mV. The first pulse inactivates the Na^+ currents and the current in response to the second pulse reflects the recovered Na^+ current fraction that is dependent on inter-pulse duration. The recovered fraction was fitted with the sum of exponentials:

$$I = A_1[1-\exp(-t/\tau_1)] + A_2[1-\exp(-t/\tau_2)] + A_3[1-\exp(-t/\tau_3)] + C,$$

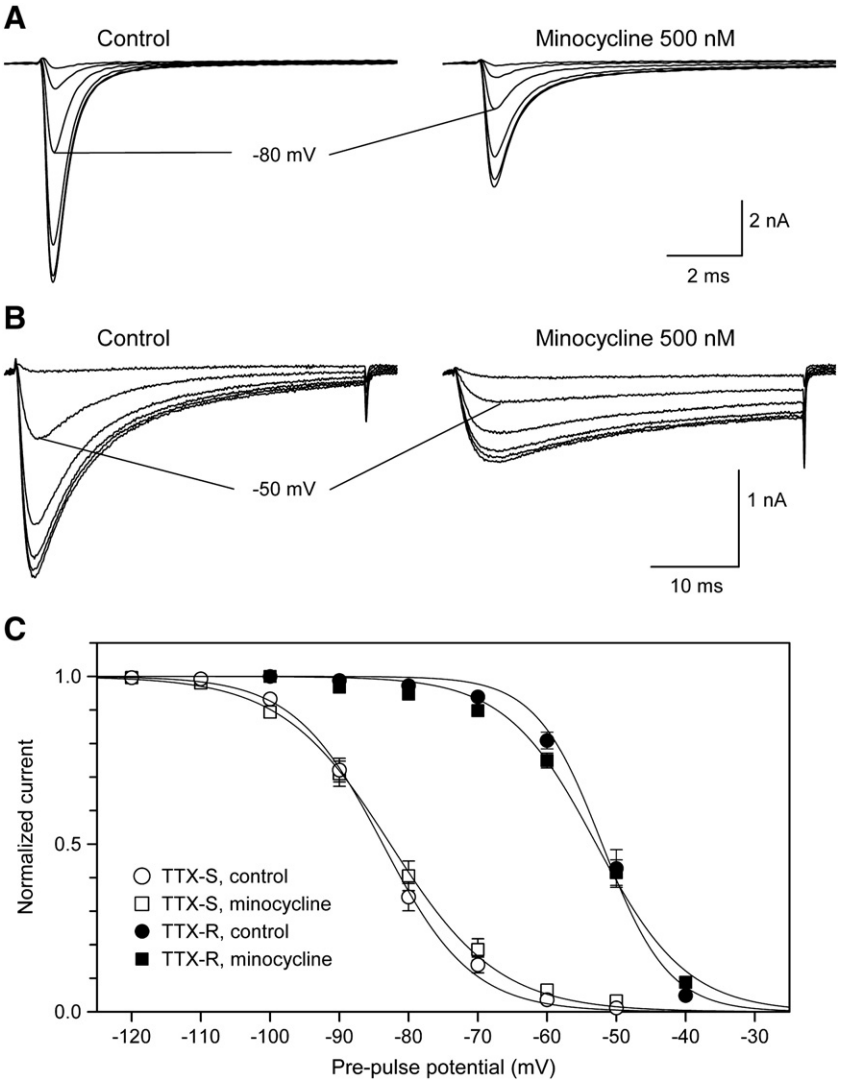

Fig. 4 – Effects of minocycline on the steady-state inactivation of Na^+ currents. Membrane potential was held at –100 mV and an inactivating pre-pulse of 10 s was given between –120 mV and –40 mV in 10-mV increments, which was immediately followed by a depolarizing pulse (A, 10 ms; B, 40 ms) to 0 mV. (A, B) Examples of TTX-S (A) and TTX-R (B) Na^+ current families obtained by this protocol before and after 10 min treatment with minocycline (500 nM). (C) Steady-state inactivation curves. Current normalized to a maximal control current was plotted against the pre-pulse potential (TTX-S, $n=8$; TTX-R, $n=8$). Curves were drawn after fit with a Boltzmann function.

where I is the current normalized to the second pulse, A_1, A_2 and A_3 are the relative proportions of each exponential, τ_1, τ_2 and τ_3 are recovery time constants, t is the inter-pulse duration in ms, and C is the proportion of the current already recovered before the measurement limit of 0.1 ms.

The recovery time courses before and after minocycline treatment (500 nM) for 10 min are shown in Fig. 5. The recovery of TTX-S Na^+ current from inactivation was best expressed as $0.89[1-\exp(-t/4.6)]+0.11[1-\exp(-t/123)]$ ($n=7$) in the control condition, and $0.79[1-\exp(-t/4.7)]+0.21[1-\exp(-t/30)]$ in the presence of minocycline. In TTX-R Na^+ current the recovery time course was best expressed as $0.42[1-\exp(-t/1.1)]+0.23[1-\exp(-t/24)]+0.15[1-\exp(-t/884)]+0.2$, with $n=8$. Minocycline greatly speeded up the recovery time course, described as $0.56[1-\exp(-t/2.3)]+0.44$.

3. Discussion

Minocycline reduced the amplitudes of both TTX-S and TTX-R Na^+ currents in rat DRG neurons at nanomolar concentration with a similar potency. Tetracycline also inhibited Na^+ currents but less potently than minocycline did. The minocycline inhibition was accompanied by a depolarizing shift in the G-V curve and an increase in its slope factor. These changes are predicted to suppress the neuronal excitability further. In nociceptive neurons TTX-S $Na_V1.7$ channels act to boost subthreshold potential bringing the cell to closer to the action potential threshold for TTX-R $Na_V1.8$ channels (Dib-Hajj et al., 2007). The depolarizing shift in the voltage dependence of activation would reduce window currents and hence the

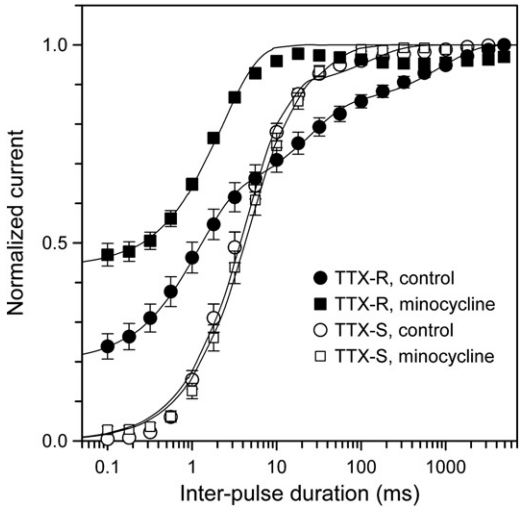

Fig. 5 – Effects of minocycline on the recovery of Na^+ currents from inactivation. Two identical pulses of 10-ms (TTX-S) or 40-ms (TTX-R) duration, to 0 mV from a holding potential of –100 mV, were separated by an inter-pulse (–100 mV) duration of increasing amount of time. The protocol was run before and after 10 min minocycline treatment (500 nM). Current in response to the second pulse was normalized and plotted as a function of the inter-pulse duration, on a logarithmic scale (TTX-S, *n* = 7; TTX-R, *n* = 8). Curves were obtained by fitting the plotted data to an exponential function.

sub-threshold potential generation. Minocycline affected the steady-state inactivation of two Na^+ currents only to a small degree. However, minocycline considerably slowed the inactivation of both Na^+ currents, and speeded up their recovery rates from inactivation. These effects should rather enhance excitability and support the high frequency firing of the sensory neurons. At micromolar concentration of minocycline, however, Na^+ currents were blocked entirely. Thus, the latter effects may be of no consequence at a higher concentration.

Our result is in sharp contrast to the study by Cho et al. (2006) showing minocycline at concentrations as high as 100 μM had no effect at all on Na^+ currents in rat DRG neurons. Their Na^+ currents, however, were mixed with K^+ currents, and were not identified as Na^+ currents using TTX or kinetic characteristics. In another study, minocycline at 100 μM blocked Na^+ current in rat hippocampal neurons by only 20%, with an IC_{50} value of 67 μM (González et al., 2007). In contrast, our results show minocycline at 3 μM almost completely blocking both TTX-S and TTX-R Na^+ currents in DRG neurons, with IC_{50} values of 350 nM and 410 nM, respectively (Fig. 2). In addition, minocycline shifted the activation voltage of hippocampal Na^+ current toward more hyperpolarizing potentials, while it produced a depolarizing shift in DRG Na^+ currents (Fig. 3). The huge difference in minocycline's potency and mode of action between these two tissues may arise from the different Na^+ channel isoforms they express. TTX-S $Na_V1.1$, $Na_V1.2$, and $Na_V1.6$ comprise hippocampal Na^+ current, whereas, in DRG neurons, $Na_V1.1$, $Na_V1.6$, and $Na_V1.7$ shape TTX-S Na^+ current, and $Na_V1.8$ and $Na_V1.9$ shape TTX-R Na^+ current (Black et al., 2004; Goldin, 2001). Alternatively, Na^+ current inhibition by minocycline may depend on cell backgrounds, which may have different machinery for modulating Na^+ channels.

Minocycline inhibition of Na^+ currents in DRG neurons with IC_{50} values at submicromolar concentrations is quite potent in its effects on membrane electrical properties. Tetracycline at clinically relevant concentrations (i.e., therapeutic serum concentrations, 7-30 μM) produces a combination of open channel and competitive block of nicotinic acetylcholine receptor transfected into HEK293 cells, with an IC_{50} value of 30 μM, which underlies the impairment of neuromuscular transmission (Schlesinger et al., 2004). In hippocampal neurons, minocycline inhibits the frequency (IC_{50}, 64 μM) and amplitude (IC_{50}, 42 μM) of spontaneous excitatory postsynaptic currents and Ca^{2+} current (IC_{50}, 45 μM), but not K^+ current or current elicited by γ-aminobutyric acid or glutamate (González et al., 2007).

Microglial activation and inflammatory mediators have been proposed to contribute to the development of chronic pain (Watkins et al., 2007). Nerve injury, inflammation, and noxious stimuli in the periphery can all increase activated microglia in the central nervous system, which in turn release pro-inflammatory cytokines and other substances that facilitate pain transmission (Coyle, 1998; Fu et al., 1999; Sweitzer et al., 1999). Minocycline is a potent inhibitor of microglial activation and proliferation, and attenuates hyperalgesia and allodynia in different models of neuropathic pain. In the spinal nerve transection model of neuropathic pain, minocycline inhibits microglial activation and suppresses pro-inflammatory cytokines such as IL-1β, IL-6, and TNF-α, at the inflicted spinal cord (Raghavendra et al., 2003). Minocycline inhibits inflammatory processes associated with the chronic constriction injury model of neuropathic pain, such as activation of microglial cells and nuclear factor κB in the dorsal horn, and serum IL-6 production (Gu et al., 2004; Zanjani et al., 2006). In the sciatic inflammatory neuropathy model, minocycline decreases microglial activation and attenuates IL-1β and TNF-α in the spinal cord (Ledeboer et al., 2005). Central nerve injuries also activate microglia, and the activated microglia contribute to the chronic pain after a spinal cord injury. Again, minocycline attenuates pain-related behaviors and microglial activation in this centrally induced pain (Hains and Waxman, 2006).

DRG neurons are primary sensory cells along the pain signaling pathways. The expression and gating properties of voltage-gated Na^+ channels in DRG neurons change in various pain states (Dib-Hajj et al., 2009; Lampert et al., 2010). In particular, $Na_V1.7$, $Na_V1.8$, and $Na_V1.9$ play roles in the establishment and maintenance of chronic inflammatory pain (Black et al., 2004; Strickland et al., 2008). Gene-deletion mutants of these channels have revealed reduced or abolished inflammatory pain responses (Akopian et al., 1999; Amaya et al., 2006; Nassar et al., 2004). Selective deletion of $Na_V1.8$, with small interfering RNAs, reverses mechanical allodynia in neuropathic rats (Dong et al., 2007). In humans, mutations in the $Na_V1.7$ gene have been linked to primary erythermalgia, paroxysmal extreme pain disorder, and channelopathy-associated insensitivity to pain (Cox et al., 2006;

Fertleman et al., 2006; Yang et al., 2004). Blockers targeting Na^+ channels in the sensory neurons can be used to treat pain. For example, one peripherally acting compound, abbreviated BZP, has a high affinity and preferential selectivity for $Na_V1.7$ over $Na_V1.8$ and $Na_V1.5$. BZP reverses hyperalgesia in inflammatory pain and allodynia in neuropathic pain in rats without any impairment of motor coordination (McGowan et al., 2009). A-887826, an $Na_V1.8$ blocker, suppresses both evoked and spontaneous action potential firing in DRG neurons from rats with inflammation and attenuates allodynia in neuropathic rats (Zhang et al., 2010). In view of the importance of Na^+ channels of DRG neurons in the pathogenesis of many different pain states, minocycline inhibition of the channels is considered to be related to its analgesic effects in addition to its inhibition of microglia in the spinal cord.

The p38 mitogen-activated protein kinases (MAPK) play an important role in nerve injury and inflammatory pain signal transduction in the DRG and spinal cord. Peripheral inflammation activates p38 via nerve growth factor in the soma of C fiber nociceptors in the DRG and increases TRPV1 channel expression, which is necessary for maintaining inflammatory heat hyperalgesia (Ji et al., 2002). Spinal nerve ligation also produces p38 activation in spinal microglia and DRG neurons, which contributes to the generation of mechanical allodynia (Jin et al., 2003). Activated p38 reduces the $Na_V1.6$ channel current by means of channel ubiquitination and internalization (Gasser et al., 2010; Wittmack et al., 2005). Contrastingly, p38 inhibition reduces both basal and TNF-α-stimulated TTX-R Na^+ currents in DRG neurons without any effect on gating properties (Jin and Gereau, 2006). In the same context, $Na_V1.8$ and p38 are co-localized in DRG neurons, and phosphorylation of $Na_V1.8$ by p38 increases $Na_V1.8$ current density (Hudmon et al., 2008). Extracellular signal-regulated kinase (ERK), another MAPK, is rapidly phosphorylated in DRG neurons after noxious stimuli, and an ERK inhibitor attenuates thermal hyperalgesia after capsaicin injection, suggesting an involvement of ERK in peripheral sensitization (Dai et al., 2002). ERK inhibition produces a depolarizing shift in the voltage dependence of both activation and steady-state inactivation of $Na_V1.7$, without altering current density (Stamboulian et al., 2010). Minocycline prevents the activation of both p38 and ERK in microglial cells (Hua et al., 2005; Nikodemova et al., 2006; Tikka and Koistinaho, 2001). If the suppression of p38 or ERK occurred in the present study, however, it seemed to contribute minimally to minocycline inhibition of TTX-S and TTX-R Na^+ currents, since two types of Na^+ currents experienced rather similar modulation, with suppression of the current amplitude, a depolarizing shift in the activation voltage, and a slowed inactivation.

Rat microglia express $Na_V1.1$, $Na_V1.5$ and $Na_V1.6$ (Black et al., 2009). In experimental autoimmune encephalomyelitis and multiple sclerosis, $Na_V1.6$ expression increases in activated microglia. Na^+ channel blockers (phenytoin and TTX) reduce the release of IL-1α, IL-1β and TNF-α from, and the migration and phagocytic function of, activated microglia (Black et al., 2009; Craner et al., 2005). Thus, Na^+ channel inhibition may participate in minocycline inhibition of microglia, by which minocycline exerts analgesia and neuroprotection.

4. Experimental procedures

4.1. *Cell preparation*

All experiments were conducted in accordance with the guidelines and the approval of the Institutional Animal Ethics Committee. DRG neurons were isolated from Sprague–Dawley rats of 2–6 days old. Rats were decapitated and the spinal column was removed. DRGs in all spinal levels were harvested and desheathed in ice-cold Ca^{2+}/Mg^{2+}-free phosphate-buffered saline (PBS, Sigma-Aldrich, St. Louis, MO). The isolated tissue was then enzymatically digested, with 0.125% collagenase first (Type II-S, Sigma-Aldrich) for 15 min, and then with 0.25% trypsin (Type XI, Sigma-Aldrich) for 10 min, both in PBS at 36 °C. The treated tissues were rinsed with a culture medium composed of 10% fetal bovine serum (J R Scientific Inc., Woodland, CA) in Dulbecco's Modified Eagle Medium (GIBCO, Grand Island, NY). Individual cells were then mechanically dissociated by triturating the DRGs through fire-polished Pasteur pipettes. The dispersed cells were plated onto glass cover slips (12-mm diameter, Marienfeld GmbH, Germany), previously coated with 0.1 mg/ml poly-L-lysine (Sigma-Aldrich), in 35-mm diameter tissue culture dishes. The dishes filled with the culture medium were maintained in a humidified incubator at 36 °C under an atmosphere of 5% CO_2. All recordings were made within 2–7 h of cell plating.

4.2. *Electrophysiological recording*

Whole cell patch-clamp recordings of Na^+ currents in the acutely dissociated rat DRG neurons were performed at room temperature (22-24 °C). Voltage was controlled using an Axopatch 200B amplifier (Axon Instruments, Union City, CA) driven from a PC, from which pulse protocols were generated and into which data were stored for off-line analysis, using Clampex 8 software (Axon Instruments) and a digital interface (Digidata 1322A, Axon Instruments). Recordings were made in solutions to select out Na^+ currents, and Na^+ gradient was reduced in order to attain a good voltage-clamp of the currents. The external solution contained (mM): NaCl 30, choline chloride 120, tetraethylammonium chloride 20, D-glucose 5, HEPES 5, $MgCl_2$ 1, $CaCl_2$ 1, and $LaCl_3$ 0.01 (pH titrated to 7.4 with tetraethylammonium hydroxide). The internal solution contained (mM): NaCl 10, CsCl 65, CsF 70, and HEPES 10 (pH titrated to 7.2 with CsOH). Patch pipettes (between 0.9 and 1.0 MΩ) were pulled from borosilicate glass capillaries (G150TF-4, Warner Instrument, Hamden, CT) with a two-step vertical puller (PP83, Narishige, Tokyo, Japan) and heat-polished with a microforge (MF83, Narishige). An Ag-AgCl pellet/3 M KCl-agar bridge was used for the reference electrode. Capacity transients were cancelled and series resistance was compensated (70–90%) with amplifier circuitry. Linear leakage currents were digitally subtracted on-line by means of P/4 routines. The liquid junction potential of −4 mV measured between internal and external solution was corrected. All recordings were started at least 10 min after establishing the whole cell configuration to allow the Na^+ current to stabilize. Currents were low-pass filtered at 5 kHz and digitally sampled at 50 kHz using Clampex 8 software.

A fast Na^+ current that inactivated within 2-3 ms at 0 mV depolarization in large-diameter neurons (>30 μm) was selected as the TTX-S Na^+ current, and its TTX sensitivity was confirmed with 100 nM TTX (Sigma-Aldrich) at the end of each experiment. TTX-R Na^+ current was recorded from small-diameter neurons (<20 μm) and isolated by eliminating TTX-S Na^+ current by including 100 nM TTX in the external solution in all experiments (Roy and Narahashi, 1992).

Minocycline and tetracycline (Sigma-Aldrich) were dissolved in dimethylsulfoxide to form 1000-fold stock solutions. Stock solutions were stored frozen at −20 °C in small aliquots and diluted in the external solution to the desired concentrations immediately before use. All salts were obtained from Sigma-Aldrich.

Data were analyzed using Clampfit 8 (Axon Instruments) and SigmaPlot 9 (Jandel Scientific, San Rafael, CA) softwares. Data are presented as means±S.E.M. and *n* refers to the number of cells examined. Student's *t*-test was used for comparisons and statistical significance was set at $P<0.05$.

Acknowledgments

This work was supported by the Korea Research Foundation Grant funded by the Korean Government (KRF-2008-314-C00251).

REFERENCES

Akopian, A.N., Sivilotti, L., Wood, J.N., 1996. A tetrodotoxin-resistant voltage-gated sodium channel expressed by sensory neurons. Nature 379, 257–262.

Akopian, A.N., Souslova, V., England, S., Okuse, K., Ogata, N., Ure, J., Smith, A., Kerr, B.J., McMahon, S.B., Boyce, S., Hill, R., Stanfa, L.C., Dickenson, A.H., Wood, J.N., 1999. The tetrodotoxin-resistant sodium channel SNS has a specialized function in pain pathways. Nat. Neurosci. 2, 541–548.

Amaya, F., Wang, H., Costigan, M., Allchorne, A.J., Hatcher, J.P., Egerton, J., Stean, T., Morisset, V., Grose, D., Gunthorpe, M.J., Chessell, I.P., Tate, S., Green, P.J., Woolf, C.J., 2006. The voltage-gated sodium channel $Na_v1.9$ is an effector of peripheral inflammatory pain hypersensitivity. J. Neurosci. 26, 12852–12860.

Amin, A.R., Attur, M.G., Thakker, G.D., Patel, P.D., Vyas, P.R., Patel, R.N., Patel, I.R., Abramson, S.B., 1996. A novel mechanism of action of tetracyclines: effects on nitric oxide synthases. Proc. Natl. Acad. Sci. USA 93, 14014–14019.

Amir, R., Argoff, C.E., Bennett, G.J., Cummins, T.R., Durieux, M.E., Gerner, P., Gold, M.S., Porreca, F., Strichartz, G.R., 2006. The role of sodium channels in chronic inflammatory and neuropathic pain. J. Pain 7, S1–S29.

Black, J.A., Liu, S., Tanaka, M., Cummins, T.R., Waxman, S.G., 2004. Changes in the expression of tetrodotoxin-sensitive sodium channels within dorsal root ganglia neurons in inflammatory pain. Pain 108, 237–247.

Black, J.A., Liu, S., Waxman, S.G., 2009. Sodium channel activity modulates multiple functions in microglia. Glia 57, 1072–1081.

Block, M.L., Hong, J.S., 2005. Microglia and inflammation-mediated neurodegeneration: multiple triggers with a common mechanism. Prog. Neurobiol. 76, 77–98.

Blum, D., Chtarto, A., Tenenbaum, L., Brotchi, J., Levivier, M., 2004. Clinical potential of minocycline for neurodegenerative disorders. Neurobiol. Dis. 17, 359–366.

Cho, I.H., Chung, Y.M., Park, C.K., Park, S.H., Li, H.Y., Kim, D., Piao, Z.G., Choi, S.Y., Lee, S.J., Park, K., Kim, J.S., Jung, S.J., Oh, S.B., 2006. Systemic administration of minocycline inhibits formalin-induced inflammatory pain in rat. Brain Res. 1072, 208–214.

Colovic, M., Caccia, S., 2003. Liquid chromatographic determination of minocycline in brain-to-plasma distribution studies in the rat. J. Chromatogr. B Anal. Technol. Biomed. Life Sci. 791, 337–343.

Cox, J.J., Reimann, F., Nicholas, A.K., Thornton, G., Roberts, E., Springell, K., Karbani, G., Jafri, H., Mannan, J., Raashid, Y., Al-Gazali, L., Hamamy, H., Valente, E.M., Gorman, S., Williams, R., McHale, D.P., Wood, J.N., Gribble, F.M., Woods, C.G., 2006. An *SCN9A* channelopathy causes congenital inability to experience pain. Nature 444, 894–898.

Coyle, D.E., 1998. Partial peripheral nerve injury leads to activation of astroglia and microglia which parallels the development of allodynic behavior. Glia 23, 75–83.

Craner, M.J., Damarjian, T.G., Liu, S., Hains, B.C., Lo, A.C., Black, J.A., Newcombe, J., Cuzner, M.L., Waxman, S.G., 2005. Sodium channels contribute to microglia/macrophage activation and function in EAE and MS. Glia 49, 220–229.

Cummins, T.R., Sheets, P.L., Waxman, S.G., 2007. The roles of sodium channels in nociception: implications for mechanisms of pain. Pain 131, 243–257.

Dai, Y., Iwata, K., Fukuoka, T., Kondo, E., Tokunaga, A., Yamanaka, H., Tachibana, T., Liu, Y., Noguchi, K., 2002. Phosphorylation of extracellular signal-regulated kinase in primary afferent neurons by noxious stimuli and its involvement in peripheral sensitization. J. Neurosci. 22, 7737–7745.

Dib-Hajj, S.D., Tyrrell, L., Black, J.A., Waxman, S.G., 1998. NaN, a novel voltage-gated Na channel, is expressed preferentially in peripheral sensory neurons and down-regulated after axotomy. Proc. Natl. Acad. Sci. USA 95, 8963–8968.

Dib-Hajj, S.D., Cummins, T.R., Black, J.A., Waxman, S.G., 2007. From genes to pain: Na_v 1.7 and human pain disorders. Trends Neurosci. 30, 555–563.

Dib-Hajj, S.D., Black, J.A., Waxman, S.G., 2009. Voltage-gated sodium channels: therapeutic targets for pain. Pain Med. 10, 1260–1269.

Djouhri, L., Newton, R., Levinson, S.R., Berry, C.M., Carruthers, B., Lawson, S.N., 2003. Sensory and electrophysiological properties of guinea-pig sensory neurones expressing $Na_v1.7$ (PN1) Na^+ channel α subunit protein. J. Physiol. 546, 565–576.

Domercq, M., Matute, C., 2004. Neuroprotection by tetracyclines. Trends Pharmacol. Sci. 25, 609–612.

Dong, X.W., Goregoaker, S., Engler, H., Zhou, X., Mark, L., Crona, J., Terry, R., Hunter, J., Priestley, T., 2007. Small interfering RNA-mediated selective knockdown of $Na_V1.8$ tetrodotoxin-resistant sodium channel reverses mechanical allodynia in neuropathic rats. Neuroscience 146, 812–821.

Fertleman, C.R., Baker, M.D., Parker, K.A., Moffatt, S., Elmslie, F.V., Abrahamsen, B., Ostman, J., Klugbauer, N., Wood, J.N., Gardiner, R.M., Rees, M., 2006. *SCN9A* mutations in paroxysmal extreme pain disorder: allelic variants underlie distinct channel defects and phenotypes. Neuron 52, 767–774.

Fu, K.Y., Light, A.R., Matsushima, G.K., Maixner, W., 1999. Microglial reactions after subcutaneous formalin injection into the rat hind paw. Brain Res. 825, 59–67.

Gasser, A., Cheng, X., Gilmore, E.S., Tyrrell, L., Waxman, S.G., Dib-Hajj, S.D., 2010. Two Nedd4-binding motifs underlie modulation of sodium channel $Na_v1.6$ by p38 MAPK. J. Biol. Chem. 285, 26149–26161.

Goldin, A.L., 2001. Resurgence of sodium channel research. Annu. Rev. Physiol. 63, 871–894.

González, J.C., Egea, J., Del Carmen Godino, M., Fernandez-Gomez, F.J., Sánchez-Prieto, J., Gandía, L., García, A.G., Jordán, J., Hernández-Guijo, J.M., 2007. Neuroprotectant minocycline depresses glutamatergic neurotransmission and Ca^{2+} signalling in hippocampal neurons. Eur. J. Neurosci. 26, 2481–2495.

Greenwald, R.A., Golub, L.M., Lavietes, B., Ramamurthy, N.S., Gruber, B., Laskin, R.S., McNamara, T.F., 1987. Tetracyclines inhibit human synovial collagenase in vivo and in vitro. J. Rheumatol. 14, 28–32.

Gu, E.Y., Han, H.S., Park, J.S., 2004. Effect of minocycline on activation of glia and nuclear factor kappa B in an animal nerve injury model. Korean J. Physiol. Pharmacol. 8, 237–243.

Hains, B.C., Waxman, S.G., 2006. Activated microglia contribute to the maintenance of chronic pain after spinal cord injury. J. Neurosci. 26, 4308–4317.

Hua, X.Y., Svensson, C.I., Matsui, T., Fitzsimmons, B., Yaksh, T.L., Webb, M., 2005. Intrathecal minocycline attenuates peripheral inflammation-induced hyperalgesia by inhibiting p38 MAPK in spinal microglia. Eur. J. Neurosci. 22, 2431–2440.

Hudmon, A., Choi, J.S., Tyrrell, L., Black, J.A., Rush, A.M., Waxman, S.G., Dib-Hajj, S.D., 2008. Phosphorylation of sodium channel $Na_v1.8$ by p38 mitogen-activated protein kinase increases current density in dorsal root ganglion neurons. J. Neurosci. 28, 3190–3201.

Ji, R.R., Samad, T.A., Jin, S.X., Schmoll, R., Woolf, C.J., 2002. p38 MAPK activation by NGF in primary sensory neurons after inflammation increases TRPV1 levels and maintains heat hyperalgesia. Neuron 36, 57–68.

Jin, X., Gereau, R.W., 2006. Acute p38-mediated modulation of tetrodotoxin-resistant sodium channels in mouse sensory neurons by tumor necrosis factor-α. J. Neurosci. 26, 246–255.

Jin, S.X., Zhuang, Z.Y., Woolf, C.J., Ji, R.R., 2003. p38 mitogen-activated protein kinase is activated after a spinal nerve ligation in spinal cord microglia and dorsal root ganglion neurons and contributes to the generation of neuropathic pain. J. Neurosci. 23, 4017–4022.

Kloppenburg, M., Verweij, C.L., Miltenburg, A.M., Verhoeven, A.J., Daha, M.R., Dijkmans, B.A., Breedveld, F.C., 1995. The influence of tetracyclines on T cell activation. Clin. Exp. Immunol. 102, 635–641.

Lampert, A., O'Reilly, A.O., Reeh, P., Leffler, A., 2010. Sodium channelopathies and pain. Pflugers Arch. 460, 249–263.

Ledeboer, A., Sloane, E.M., Milligan, E.D., Frank, M.G., Mahony, J.H., Maier, S.F., Watkins, L.R., 2005. Minocycline attenuates mechanical allodynia and proinflammatory cytokine expression in rat models of pain facilitation. Pain 115, 71–83.

McGowan, E., Hoyt, S.B., Li, X., Lyons, K.A., Abbadie, C., 2009. A peripherally acting $Na_v1.7$ sodium channel blocker reverses hyperalgesia and allodynia on rat models of inflammatory and neuropathic pain. Anesth. Analg. 109, 951–958.

Narita, M., Yoshida, T., Nakajima, M., Narita, M., Miyatake, M., Takagi, T., Yajima, Y., Suzuki, T., 2006. Direct evidence for spinal cord microglia in the development of a neuropathic pain-like state in mice. J. Neurochem. 97, 1337–1348.

Nassar, M.A., Stirling, L.C., Forlani, G., Baker, M.D., Matthews, E.A., Dickenson, A.H., Wood, J.N., 2004. Nociceptor-specific gene deletion reveals a major role for $Na_v1.7$ (PN1) in acute and inflammatory pain. Proc. Natl. Acad. Sci. USA 101, 12706–12711.

Nikodemova, M., Duncan, I.D., Watters, J.J., 2006. Minocycline exerts inhibitory effects on multiple mitogen-activated protein kinases and $I\kappa B\alpha$ degradation in a stimulus-specific manner in microglia. J. Neurochem. 96, 314–323.

Pruzanski, W., Greenwald, R.A., Street, I.P., Laliberte, F., Stefanski, E., Vadas, P., 1992. Inhibition of enzymatic activity of phospholipases A_2 by minocycline and doxycycline. Biochem. Pharmacol. 44, 1165–1170.

Raghavendra, V., Tanga, F., DeLeo, J.A., 2003. Inhibition of microglial activation attenuates the development but not existing hypersensitivity in a rat model of neuropathy. J. Pharmacol. Exp. Ther. 306, 624–630.

Roy, M.L., Narahashi, T., 1992. Differential properties of tetrodotoxin-sensitive and tetrodotoxin-resistant sodium channels in rat dorsal root ganglion neurons. J. Neurosci. 12, 2104–2111.

Schlesinger, F., Krampfl, K., Haeseler, G., Dengler, R., Bufler, J., 2004. Competitive and open channel block of recombinant nAChR channels by different antibiotics. Neuromuscul. Disord. 14, 307–312.

Stamboulian, S., Choi, J.S., Ahn, H.S., Chang, Y.W., Tyrrell, L., Black, J.A., Waxman, S.G., Dib-Hajj, S.D., 2010. ERK1/2 mitogen-activated protein kinase phosphorylates sodium channel $Na_v1.7$ and alters its gating properties. J. Neurosci. 30, 1637–1647.

Stirling, D.P., Koochesfahani, K.M., Steeves, J.D., Tetzlaff, W., 2005. Minocycline as a neuroprotective agent. Neuroscientist 11, 308–322.

Strickland, I.T., Martindale, J.C., Woodhams, P.L., Reeve, A.J., Chessell, I.P., McQueen, D.S., 2008. Changes in the expression of $Na_V1.7$, $Na_V1.8$ and $Na_V1.9$ in a distinct population of dorsal root ganglia innervating the rat knee joint in a model of chronic inflammatory joint pain. Eur. J. Pain 12, 564–572.

Sweitzer, S.M., Colburn, R.W., Rutkowski, M., DeLeo, J.A., 1999. Acute peripheral inflammation induces moderate glial activation and spinal IL-1β expression that correlates with pain behavior in the rat. Brain Res. 829, 209–221.

Tikka, T.M., Koistinaho, J.E., 2001. Minocycline provides neuroprotection against *N*-methyl-D-aspartate neurotoxicity by inhibiting microglia. J. Immunol. 166, 7527–7533.

Tilley, B.C., Alarcon, G.S., Heyse, S.P., Trentham, D.E., Neuner, R., Kaplan, D.A., Clegg, D.O., Leisen, J.C., Buckley, L., Cooper, S.M., Duncan, H., Pillemer, S.R., Tuttleman, M., Fowler, S.E., 1995. Minocycline in rheumatoid arthritis. A 48-week, double-blind, placebo-controlled trial. MIRA Trial Group. Ann. Intern. Med. 122, 81–89.

Watkins, L.R., Hutchinson, M.R., Milligan, E.D., Maier, S.F., 2007. "Listening" and "talking" to neurons: implications of immune activation for pain control and increasing the efficacy of opioids. Brain Res. Rev. 56, 148–169.

Wittmack, E.K., Rush, A.M., Hudmon, A., Waxman, S.G., Dib-Hajj, S.D., 2005. Voltage-gated sodium channel $Na_v1.6$ is modulated by p38 mitogen-activated protein kinase. J. Neurosci. 25, 6621–6630.

Yang, Y., Wang, Y., Li, S., Xu, Z., Li, H., Ma, L., Fan, J., Bu, D., Liu, B., Fan, Z., Wu, G., Jin, J., Ding, B., Zhu, X., Shen, Y., 2004. Mutations in *SCN9A*, encoding a sodium channel alpha subunit, in patients with primary erythermalgia. J. Med. Genet. 41, 171–174.

Yong, V.W., Wells, J., Giuliani, F., Casha, S., Power, C., Metz, L.M., 2004. The promise of minocycline in neurology. Lancet Neurol. 3, 744–751.

Yrjänheikki, J., Tikka, T., Keinänen, R., Goldsteins, G., Chan, P.H., Koistinaho, J., 1999. A tetracycline derivative, minocycline, reduces inflammation and protects against focal cerebral ischemia with a wide therapeutic window. Proc. Natl. Acad. Sci. USA 96, 13496–13500.

Zanjani, T.M., Sabetkasaei, M., Mosaffa, N., Manaheji, H., Labibi, F., Farokhi, B., 2006. Suppression of interleukin-6 by minocycline in a rat model of neuropathic pain. Eur. J. Pharmacol. 538, 66–72.

Zhang, X.F., Shieh, C.C., Chapman, M.L., Matulenko, M.A., Hakeem, A.H., Atkinson, R.N., Kort, M.E., Marron, B.E., Joshi, S., Honore, P., Faltynek, C.R., Krafte, D.S., Jarvis, M.F., 2010. A-887826 is a structurally novel, potent and voltage-dependent $Na_v1.8$ sodium channel blocker that attenuates neuropathic tactile allodynia in rats Neuropharmacology 59, 201–207.